Neutrino Recoil Spectrometer. Investigation of A^{37}

O. KOFOED-HANSEN*
Institute for Theoretical Physics, University of Copenhagen, Copenhagen, Denmark
(Received July 9, 1954)

A neutrino recoil spectrometer has been constructed. The recoil momentum and the charge distribution of the recoil ions from the K capture of A^{37} has been studied. The results are: neutrino energy, (812±8) kev; recoils of charge 1, (26±3) percent; recoils of charge 2, (13±4) percent; recoils of charge 3, (38±4) percent; recoils of charge 4, (18±2) percent; recoils of charge 5, (4±1) percent; and recoils of charge 6, (1±1) percent. Furthermore, the average momentum of the electrons emitted during the ionization of the recoils is 69±1 gauss-cm. The most energetic Auger electrons have a momentum of 162±4 gauss-cm and they occur in (65±5) percent of the decays.

INTRODUCTION

MANY recoil experiments have successfully demonstrated that momentum is missing in β decay and K capture if the neutrino is not postulated.[1] Important information about the angular correlation in β decay has also been obtained.[2] On the other hand, such experiments have so far not given very precise numerical results. The present paper describes a method which at least in principle makes very high precision measurements possible. The instrument permits a study of the motion of recoil ions in crossed electric and magnetic fields. The recoil ions are detected by the current they produce when hitting the detector plates. The main features of the method have been described previously.[3]

THEORY OF THE INSTRUMENT

In principle, the instrument consists of a set of plane parallel condenser plates adjusted so that the magnetic field is parallel to the surface of the plates. The decaying atoms form a gas which decays uniformly inside the volume of the condenser. The current of recoils and electrons going to the plates is measured as a function of the electric field F and the magnetic field H. If H is larger than F, the orbits are always periodic in the direction parallel to F. If $2a$ is the distance between the plates (see Fig. 1), an ion of charge z, mass M, initial velocity u, and starting point x_0 will have the extrema of its orbit $x^{\max}$ and $x^{\min}$, given by

$$\left.\begin{matrix}\omega a\\ -Wa\end{matrix}\right\}=\left.\begin{matrix}x^{\max}\\ x^{\min}\end{matrix}\right\}-x_0=Ba\{1+A\sin\theta\cos\varphi \pm[1+2A\sin\theta\cos\varphi+A^2\sin^2\varphi]^{\frac{1}{2}}\},\quad(1)$$

where θ is the angle between $M\mathbf{u}$ and $\mathbf{H}$ and φ is the azimuth of $M\mathbf{u}$ measured from the y axis. [See reference 3, Eqs. (38) and (40).] We use the abbreviations

$$\mathcal{A}=A\sin\theta=(2aHu/Vc)\sin\theta,\quad(2a)$$

$$B=(2Mc^2V)/[(2aH)^2z],\quad(2b)$$

$$V=2aF.\quad(2c)$$

We also introduce the relative amplitude in the motion

$$L=\omega+W.\quad(2d)$$

The functions ω and W are shown in Fig. 2 as functions of φ in the special case $\mathcal{A}=1$, $B=1$. If $L>2$, no particles can spiral out of the condenser. They will either hit plate 1 or plate 2. When $L<2$, $\frac{1}{2}(2-L)$ particles will spiral out. Let us denote by φ', $0\leqslant\varphi'\leqslant\pi$, the angle where $L=2$, i.e.,

$$\varphi'=\begin{cases}0 & \text{for } B<1/(1+\mathcal{A}),\\ \arccos\left[\dfrac{1}{2\mathcal{A}}\left(\dfrac{1}{B^2}-1-\mathcal{A}^2\right)\right] & \text{for } \dfrac{1}{1+\mathcal{A}}<B<\dfrac{1}{1-\mathcal{A}},\\ \pi & \text{for } B>1/(1-\mathcal{A});\end{cases}\quad(3)$$

when no such angle exists the proper limits 0 or π are given. Furthermore, it is assumed that $V>\frac{1}{2}Mu^2$, which ensures that the function $W<2$.

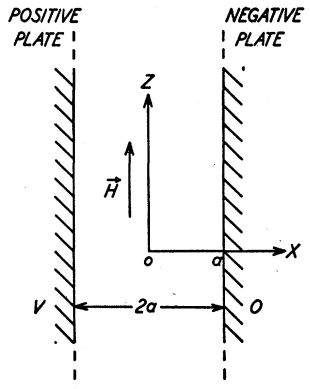

FIG. 1. Principle of the instrument.

*Present address: Columbia University, New York, N Y.
[1] See O. Kofoed-Hansen, Physica **18**, 1287 (1952).
[2] B. M. Rustad and S. L. Ruby, Phys. Rev. **89**, 880 (1953); J. S. Allen and W. K. Jentschke, Phys. Rev. **89**, 902 (1953).
[3] O. Kofoed-Hansen, Kgl. Danske Videnskab. Selskab, Mat.-fys. Medd. **26**, No. 8 (1951).

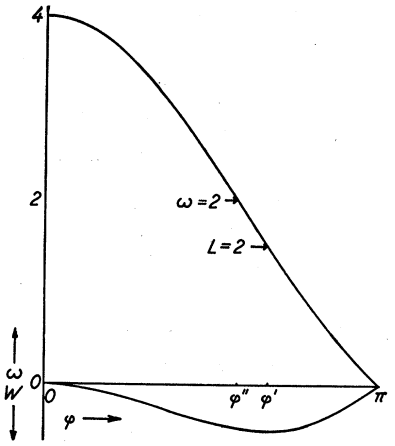

FIG. 2. The functions $\omega(\varphi)$ and $W(\varphi)$ for $\mathcal{A}=1$ and $B=1$.

When $\omega>2$, all particles starting out towards the attracting plate will hit this plate, but when $\omega<2$ some may miss this plate and either hit the repelling plate or spiral out. Let us denote by φ'', $0\leqslant\varphi''\leqslant\pi$, the angle where $\omega=2$, i.e.,

$$\varphi''=\begin{cases}0 & \text{for } B<1/(1+\mathcal{A}),\\ \arccos\left[\dfrac{2}{B\mathcal{A}}-\left[\dfrac{4}{B\mathcal{A}^2}+1\right]^{\frac{1}{2}}\right] & \\ & \text{for } \dfrac{1}{1+\mathcal{A}}<B<\dfrac{1}{1-\mathcal{A}},\\ \pi & \text{for } B>1/(1-\mathcal{A}).\end{cases} \tag{4}$$

For specific values of A and B the relative number of particles spiraling out will, therefore, be given by

$$g(A,B)=\int_0^{\frac{1}{2}\pi}\sin\theta d\theta\int_{\varphi'}^{\pi}(2-L)d\varphi/2\pi$$
$$=\int_0^{\frac{1}{2}\pi}\sin\theta\left\{\frac{\pi-\varphi'}{\pi}-\frac{2B}{\pi}[E(k,\tfrac{1}{2}\pi)-E(k,\tfrac{1}{2}\varphi')](1+\mathcal{A})\right\}d\theta. \tag{5}$$

The number hitting the repelling plate is given by

$$h(A,B)=\tfrac{1}{2}\int_0^{\frac{1}{2}\pi}\left[\int_0^{\pi}W\frac{d\varphi}{2\pi}+\int_{\varphi''}^{\pi}(2-\omega)\frac{d\varphi}{2\pi}-\int_{\varphi'}^{\pi}(2-L)\frac{d\varphi}{2\pi}\right]\sin\theta d\theta$$
$$=\frac{B}{4\pi}\int_0^{\frac{1}{2}\pi}\sin\theta\{(1+\mathcal{A})[4E(k,\tfrac{1}{2}\pi)-4E(k,\tfrac{1}{2}\varphi')+2E(k,\tfrac{1}{2}\varphi'')]-2\pi+\varphi''+(2/B)\times(\varphi'-\varphi'')+\mathcal{A}\sin\varphi''\}d\theta, \tag{6}$$

and the number hitting the attracting plate is given by

$$f(A,B)=1-g(A,B)-h(A,B), \tag{7}$$

where

$$E(k,\varphi)=\int_0^{\varphi}(1-k^2\sin^2t)^{\frac{1}{2}}dt, \tag{8}$$

$$k^2=4\mathcal{A}/(1+\mathcal{A})^2. \tag{9}$$

When the particles have initially a distribution in velocity, the functions f, g, and h have to be integrated over this distribution. Since $A\sim u$, such an integration is essentially an integration over A. If there is a distribution in z, one has to sum over this distribution; since only B contains z, this will be a summation over B. In the case of A^{37} we can primarily confine ourselves to a distribution in z. In such a case the currents going to the two plates and the currents spiraling out are given below. The current will of course also contain a component from the electrons. However, in the present experiments we are mainly dealing with such values of H and F that the approximation in Eq. (49) of reference 3 can be used. Thus we get for the total current to the positive plate (S_z is the charge distribution function and N the total number of disintegrations):

$$i_+\cong\sum_z[S_z\cdot zh(A,B)Ne]-Ne\langle z\rangle\tfrac{1}{4}\pi c\langle p_e\rangle/(2aHe), \tag{10}$$

and to the negative plate:

$$i_-\cong\sum_z[S_z\cdot zf(A,B)Ne]-Ne\langle z\rangle\tfrac{1}{4}\pi c\langle p_e\rangle/(2aHe). \tag{11}$$

LIMITING CASES

The above formulas take especially simple forms in the two cases:

$$B>1/(1-A),\quad A<1; \tag{12}$$

$$B<1/(1+A),\quad A<1. \tag{13}$$

One finds in case (12),

$$h(A,B)\cong\frac{B}{2}\left\{\frac{A^2}{12}+\frac{A^4}{240}+\frac{A^6}{1120}+\frac{5A^8}{16\,128}+\cdots\right\}, \tag{14}$$

$$g(A,B)\equiv 0. \tag{15}$$

Physically, this implies that no particles can spiral out, and one is led to the approximate formulas (50) and (51) of reference 3 for i_+ and i_-. In case (13) one obtains similarly

$$h(A,B)\cong B\left\{\frac{A^2}{12}+\frac{A^4}{240}+\frac{A^6}{1120}+\frac{5A^8}{16\,128}+\cdots\right\}, \tag{16}$$

$$g(A,B)=1-B-2h(A,B). \tag{17}$$

Condition (13) means that $L<2$, i.e., that the largest orbit can lie in the space between the plates. In both these cases the integrations over a possible velocity distribution and the summations over a possible charge distribution can be carried out especially easily. The

final result will depend upon simple average values of z, p, E, etc., for the recoils.

DECAY OF A^{37}

A^{37} is reported to decay into Cl^{37} by 92 percent K capture and 8 percent L capture, with a half-life of 34 days. Primarily electrically neutral Cl^{37} atoms are formed, but successive Auger effects and the charge change of the nucleus from $Z=18$ to $Z=17$ cause a considerable ionization to take place within very short time ($\sim 10^{-10}$ sec) after the decay. The $Cl^{37}(p,n)A^{37}$ threshold shows that 816 ± 4 kev is available for the K capture.

The recoil velocity distribution is primarily a sharp line originating from the practically monoenergetic neutrino emission, but smeared out by ~ 6 percent due to the recoil from the Auger effect and by a similar amount due to the Brownian motion at STP.

This spread will cause a difference of only ~ 2 kev between $c[\langle p^2\rangle]^{\frac{1}{2}}$ and $c\langle p\rangle$, and we can therefore neglect the spread in all our expressions and apply the sharp line formulas (10) and (11), using simply $\langle u\rangle$ in these expressions instead of u. Actually, the velocity distribution could in principle be determined by the experiment, but the present experiments have been carried out at such values of V and H that primarily the charge spectrum has been investigated.

The A^{37} is produced carrier-free by $Ca(n,\alpha)$ in the Harwell pile and sent to Copenhagen enclosed in Ca. It is introduced in the sealed-off vacuum of the instrument by evaporating the Ca inside the vacuum system. Another Ca furnace in the vacuum system keeps the pressure in the instrument at 10^{-5} to 10^{-3} mm Hg for a month, the pressure being initially low and gradually increasing.

THE INSTRUMENT

A diagram of the instrument is shown in Fig. 3. An approximately homogeneous magnetic field is obtained by using a solenoidal coil surrounded by iron. The coils are watercooled and wound with 20 mm by 1 mm flat

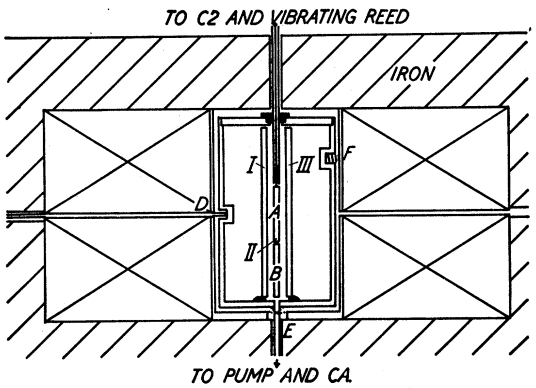

FIG. 3. Diagram of the instrument. The distance between the plates is $2a=0.704$ cm.

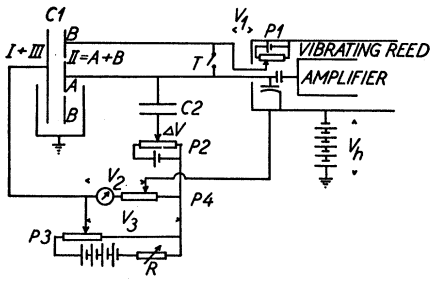

FIG. 4. Circuit diagram.

Cu wire insulated with polystyrene. The inhomogeneities amount to ~ 2 percent close to the pole pieces. The only advantage of this construction is that it is relatively inexpensive. As disadvantages appear the facts that too little space is left for introducing instruments into the field and that thereby some difficulties in handling the equipment occur. Also the field is not as homogeneous as might be desired. Even more troublesome is the fact that the temperature of the vacuum chamber is seriously affected by the heating up of the coils. Therefore an extra watercooled shield is introduced between the coils and the vacuum chamber. Temperature changes of the vacuum chamber influence the concentration of A^{37} between the collector plates.

The vacuum chamber contains a double set of condenser plates. The duplication is used for convenience in the construction only. The central part A of the central condenser plate is electrically insulated from the remainder of the plate, and is connected through a vacuum seal to a vibrating reed electrometer and to an extra condenser $C2$ of the order of 60 cm. $C2$ is placed in vacuum in order to avoid currents from cosmic ray ionization in $C2$. The second plate of $C2$ is connected to a potentiometer so that the vibrating reed electrometer is used as zero indicator only. The current to A is measured by measuring the time t it takes to charge $C2$ to 1 volt.

In order to eliminate temperature drift and changes in concentration due to the decay of A^{37}, measurements have been made by comparing the currents for given values of V and H to the current i_- obtained at $H=2500$ gauss and $V=30$ volts. This latter current is in the following put equal to unity.

The outer part B of the central condenser plate acts as a guard ring and is kept at the same potential as the collector plate A. Nevertheless contact potentials may cause small currents over the many insulators between A and B, and especial care was taken to find insulators which at the same time were sufficiently rigid mechanically and gave sufficiently good insulation even when heavily irradiated with x-rays. Textolite was found to fulfil these conditions.

The outer condenser plates are connected to a group of dry cells in the manner shown in Fig. 4. The potentiometer $P1$ determines the potential V_1 on A and B.

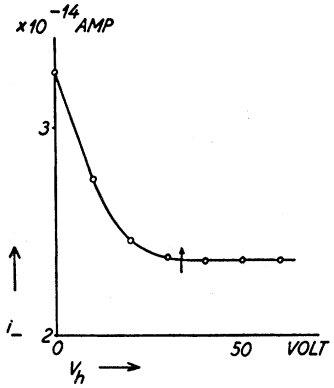

FIG. 5. The current i_- as a function of V_h for definite values of V and H.

V_1 is made equal to the contact potential between the reed and anvil in the vibrating reed electrometer. Thereby the reed indicates zero potential. When the short circuit T is removed, the instrument is ready for a measurement. *P2* gives a compensating potential on *C2*. This potential can be varied from 0 to 1 volt and is used to keep the reed showing zero and defines the time measurement for a 1-volt raise of *C2* mentioned above. *P3* gives the possibility of generating a variable potential V_3 between the outer plate (I+III) and the inner plate (II) of the instrument. V_3 can be adjusted for long-time drift by the variable resistance R. *P4* divides V_3 so that a certain portion of V_3 is connected to *C2*, and only the remainder V_2 is the main potential between I and III on the one hand and II on the other hand of the collector system *C1*. *P4* is adjusted so that a variation of V_3 causes no indication on the reed. In this way the influence on the current measurement of short- and long-time variations in V_3 is eliminated, and the measurement can be carried out at an electric potential $V=V_2-V_1$ across *C1*. When V is positive, almost all recoils hit A and electrons move in helical orbits towards the top and the bottom of the vacuum chamber. However, if the electron energy is small and if the electron is created at a positive potential, it cannot move up or down towards the chamber

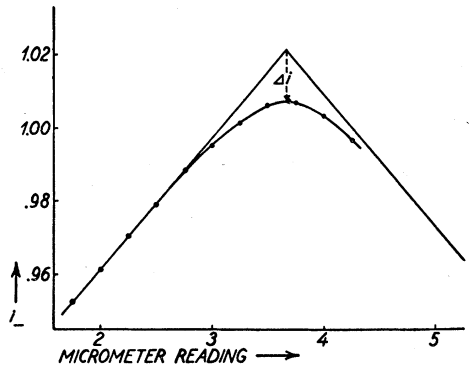

FIG. 6. The current i_- as a function of the micrometer reading. One unit micrometer reading corresponds to a tilting of the instrument of 25′.

wall but will travel to and fro in the instrument until it ionizes some gas molecule in the residual gas, thus giving a positive ion which adds to the current to A. In order to eliminate this effect the potential V_h is introduced. V_h lifts *C1* up to such a potential that all electrons can reach the walls of the instrument. This is illustrated by the measurements in Fig. 5. The figure shows the variation of i_- as a function of V_h for definite values of V and H. When $V_h>V$ the pressure effect is reduced to zero. As regards the magnetic field, the most important feature is that the field shall be parallel to the plane of the plates of *C1*. If this is not so, secondary electrons from the walls may spiral up and hit the collector system, reducing the current going to A. The setting of the plane of *C1* parallel to H is carried out by means of the micrometer screw D, the pivots E, and the phosphorbronze spring F in Fig. 3. Figure 6 shows the results of current measurements as a function of the micrometer reading. It is seen that the best possible setting of the instrument is easily found. Still the field is not strictly homogeneous and the plates are only plane to within 0.02 mm. Therefore some secondary electrons will still hit the plates. This effect is relatively small and, as we shall see later, fairly well represented by the extrapolated current Δi in Fig. 6. Inside the limits of errors, Δi is found to be constant, i.e., independent of H and V, at least in the region used in the present experiment. However, in the present instrument the field inhomogeneities produce the largest systematic error.

MEASUREMENTS

The currents illustrated in the following have been measured at various pressures from 9×10^{-6} mm Hg and upwards, and an extrapolation to zero pressure has been carried out. This correction amounts to at most 1 percent. When i_- is measured as a function of H for $V=60$ volts, the results shown in Fig. 7 are obtained. For 0.4×10^{-3} gauss$^{-1}<1/H<2\times10^{-3}$ gauss^{-1}, the curve follows the expression

$$i_-\cong Ne\langle z\rangle - Ne\langle T_R\rangle/6V - Ne\langle z\rangle[\pi\langle p_e c\rangle/(8aHe) - \langle E_e\rangle Ve/(2aHe)^2], \quad (18)$$

where $\langle T_R\rangle$ is the average kinetic energy of the recoil ions; i.e., the extrapolated line cuts $1/H=0$ in the contribution from the recoils only; this contribution is represented by the first two terms in (18). The measurement has been carried out for different V values (see Fig. 9). Thereby $Ne\langle z\rangle$ can be obtained. The result is

$$Ne\langle z\rangle = 1.071\pm0.001, \quad (19)$$

in our current units. Thus we find from Fig. 7,

$$\langle p_e\rangle = 69\pm1 \text{ gauss-cm}. \quad (20)$$

If no electrons of momentum $p\gtrsim80$ gauss-cm exist, the curve should proceed along the slightly curved line A in Fig. 7. The deviation shows that electrons exist which get a radius of curvature in their helical orbit which is

larger than a. From the behavior of the curve, one finds that the momentum of these electrons is 162 ± 4 gauss-cm; their relative number also can be estimated. If we take into account the result (22), we find that 65 ± 5 percent of the decays lead to Auger electrons of this momentum, i.e., of energy 2320 ± 120 ev. In this way the contribution to the currents from the electrons is completely accounted for; in the following figure, we correct for this contribution and for the tilting effect Δi mentioned in connection with Fig. 6. The deviation from the extrapolated curve in Fig. 7 for $1/H<0.4\times10^{-3}$ gauss is illustrated in more detail in Fig. 8. This figure has been corrected in the above-mentioned manner so that only the contribution to i_- from the recoils is given.

Within the limits of error this contribution is a constant until H becomes so strong that particles begin to miss the negative plate and either spiral out or hit the positive plate. The curve gives information about the relative numbers of highly charged particles and of the

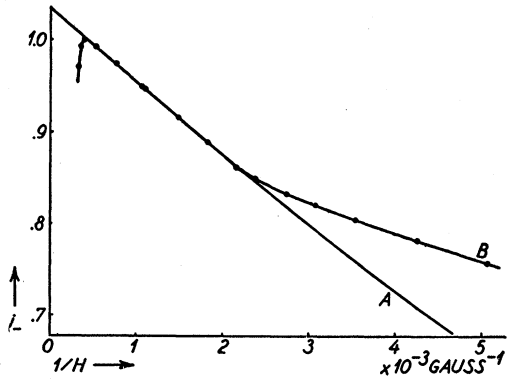

FIG. 7. The current i_- as a function of $1/H$ for $V=60$ volts and $V_h=70$ volts.

momentum of the recoils. The data are fitted to

$$\begin{aligned}\langle Muc\rangle&=(812\pm8)\text{ kev},\\ S_6&=(1\pm1)\text{ percent},\\ S_5&=(4\pm1)\text{ percent},\\ S_4&=(18\pm2)\text{ percent},\\ S_3&=(38\pm4)\text{ percent}.\end{aligned}\tag{21}$$

Since electrically neutral particles are not detected, S_0 has arbitrarily been put equal to zero, and all which is said here refers to charged recoils only.

Further analysis of i_- for higher values of H leads to rather inaccurate values for S_1 and S_2. In order to obtain more accurate information about these quantities, it is desirable to measure i_+ as a function of V. The results are shown in Fig. 9. From the slope of the curve, $N\langle T_R\rangle$ can be found. As mentioned previously, a knowledge of $\langle Muc\rangle$ gives $\langle T_R\rangle$ with sufficient accuracy; thus N can be obtained. The result is

$$Ne=0.405\pm0.008,\tag{22}$$

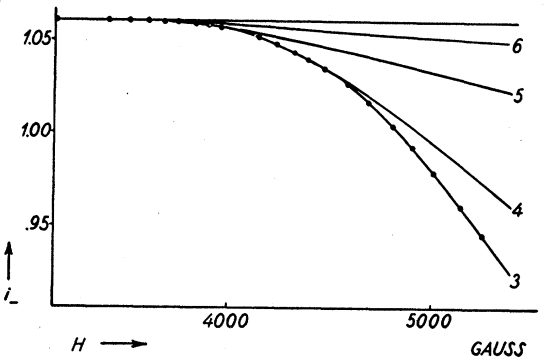

FIG. 8. Recoil contribution to i_- as a function of H.

which together with (19) and (21) gives

$$\begin{aligned}S_1&=(26\pm3)\text{ percent},\\ S_2&=(13\pm4)\text{ percent},\\ \langle z\rangle&=2.64\pm0.08.\end{aligned}$$

If no singly charged recoils of energy greater than 4 ev existed, the curve in Fig. 9 should follow curve A. The deviation gives the independent determination of

$$\begin{aligned}\langle T_R\rangle&=(10\pm1)\text{ ev},\\ S_1&=(25\pm3)\text{ percent}.\end{aligned}$$

The results thus obtained have been tested by measuring at other V, H values, and all curves so obtained have agreed with the above results. It should also be noted that all currents have been accounted for by performing the correction Δi for the tilting of the instrument; the accuracy is in this way found to be 0.001 of our units of current.

CONCLUSIONS

The experimental results obtained give a slightly lower value for the average charge than that reported by others.[4] This is without doubt connected with the fact

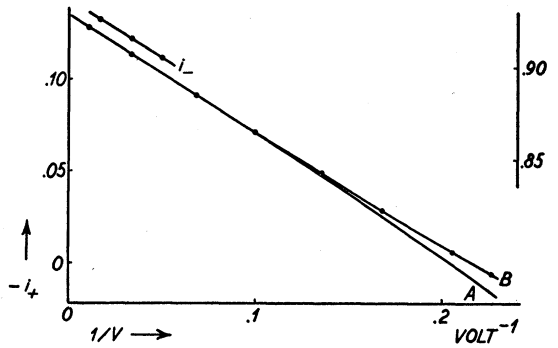

FIG. 9. The currents i_+ and i_- as functions of $1/V$. For i_+ the scale is to the left and for i_- the scale is to the right. The measurements are made at $H=675$ gauss.

[4] M. L. Perlman and J. A. Miskel, Phys. Rev. **91**, 899 (1953); S. Wexler, Phys. Rev. **93**, 182 (1954).

that it is usually assumed that 85 percent of the decays lead to the energetic Auger transitions, whereas only 65 percent are observed. It is possible that an understanding of this can be obtained by considering a little more in detail the process in which initially a K electron in A^{37} is captured, but where the resulting Cl^{37} atom is formed with a vacancy in the L shell due to the radial correlation between the electrons.[5]

[5] P. Benoist-Gueutal, Ann. Physik 8, 593 (1953).

The author wishes to express his thanks to Professor N. Bohr for his interest in this work. I am also grateful to Mr. A. Nielsen for valuable assistance in the experimental work. A detailed description of the instrument and the results obtained with A^{37} will appear in Kgl. Danske Videnskab. Selskab, Mat.-fys. Medd. A discussion of the charge spectrum together with radius of K to L capture and Auger probabilities will be given by A. Winther.

PHYSICAL REVIEW VOLUME 96, NUMBER 4 NOVEMBER 15, 1954

Energy Levels in $_{66}Dy^{160}$†

V. KESHISHIAN, H. W. KRUSE, R. J. KLOTZ, AND C. M. FOWLER
Kansas State College, Manhattan, Kansas

(Received May 26, 1954)

An energy level diagram for $_{66}Dy^{160}$ is proposed which is consistent with most of the experimental data on this activity, as well as with further data reported here. Levels are proposed at 86.2, 282, 496, 962, 1196, 1259, 1352, and 1532 kev. Beta spectra of 851±10, 557±15, 461±20, and 280±40 kev have been observed and support the diagram.

INTRODUCTION

NEUTRON capture in Tb^{159} leads to Tb^{160} which then decays by beta-minus emission to Dy^{160}. In common with several other even-even nuclear products around this mass number region, a relatively large number of conversion groups were observed by early investigators.[1] Subsequent investigations[2,3] have consistently increased the number of observed transitions, particularly in the higher-energy regions. Reports on the accompanying beta spectra have also varied, not only as to the number and intensities of the spectra, but also in the end-point values. Burson *et al.*[4] recently have summarized in some detail the available information on this activity. In addition, they have reported some new information and have proposed an energy level diagram. In this investigation, additional information has been obtained which suggests a different diagram.

EXPERIMENTAL RESULTS

Gamma Rays

More than seventy gamma rays have so far been observed and classified as to energy. These radiations were detected both through their conversion electrons and by photoelectric analysis, employing lead, tin, and molybdenum radiators. Over eighty beta-ray spectrographic plates have been taken so far with exposure times ranging from a few minutes to several weeks. Magnetic fields ranging from 100 to 800 gauss were used.

Of the many gamma rays observed, twenty-nine of the more intense lines have been incorporated into the decay scheme of Fig. 1, and are presented in Table I.

Beta Spectra

Figure 2 shows a plot of the normalized electron spectrum of Tb^{160} obtained at about 1 percent resolution. The portion of the spectrum below 150 kev is omitted since the density of the source, with backing, was of the order of a few milligrams per square centimeter. Comparison of this source density with those studied by Shull[5] indicates that source scattering effects become noticeable for energies around and below this value.

As remarked earlier, reports on the Tb^{160} beta spectra have shown considerable disagreement among various writers. It is felt here that the major cause of this lack of consistency arises from the presence of a large number of previously unrecognized weak conversion groups superimposed upon the continuous spectrum. Several different runs of the spectrum of Fig. 2, in the 300- to 800-kev region, consistently showed clusters of points several percent too high to allow fitting them with a smooth beta-spectrum type curve. Subsequent observation of spectrographic plates revealed weak conversion groups in the vicinity of all such high point regions. For example, in the region

† Sponsored by the U. S. Atomic Energy Commission.
[1] Cork, Shreffler and Fowler, Phys. Rev. 74, 240 (1948).
[2] Cork, Branyan, Rutledge, Stoddard, and LeBlanc, Phys. Rev. 78, 304 (1950).
[3] Burson, Blair, and Saxon, Phys. Rev. 77, 403 (1950).
[4] Burson, Jordon, and LeBlanc, Phys. Rev. 94, 103 (1954).
[5] F. B. Shull, Phys. Rev. 74, 917 (1948).